



## Article

# Impact of Subsurface Drainage System Design on Nitrate Loss and Crop Production

Soonho Hwang <sup>1</sup>, Shailendra Singh <sup>1</sup>, Rabin Bhattarai <sup>1,\*</sup> , Hanseok Jeong <sup>2</sup> and Richard A. Cooke <sup>1</sup>

<sup>1</sup> Department of Agricultural and Biological Engineering, University of Illinois at Urbana-Champaign, 1304 W Pennsylvania Ave, Urbana, IL 61801, USA; soonho@illinois.edu (S.H.); ss33@illinois.edu (S.S.); rcooke@illinois.edu (R.A.C.)

<sup>2</sup> Department of Environmental Engineering, Seoul National University of Science and Technology, Seoul 01811, Republic of Korea; hanjeong@seoultech.ac.kr

\* Correspondence: rbhatta2@illinois.edu

**Abstract:** Subsurface (or tile) drainage offers a valuable solution for enhancing crop productivity in poorly drained soils. However, this practice is also associated with significant nutrient leaching, which can contribute to water quality problems at the regional scale. This research presents the findings from a 4-year tile depth and spacing study in central Illinois that included three drain spacings (12.2, 18.3, and 24.4 m) and two drain depths (0.8 and 1.1 m) implemented in six plots under the corn and soybean rotation system (plots CS-1 and CS-3: 12.2 m spacing and 1.1 m depth, plots CS-2 and CS-4: 24.4 m spacing and 1.1 m depth, and plots CS-5 and CS-6 18.3 m spacing and 0.8 m depth). Our observations indicate that drain flow and NO<sub>3</sub>-N losses were higher in plots with narrower drain spacings, while plots with wider drain spacing showed reduced drain flow and NO<sub>3</sub>-N losses. Specifically, plots set up with drain spacings of 18.3 m and 24.4 m showed significant reductions in drain flow compared to plots featuring a 12.2 m drain spacing. Likewise, plots characterized by 18.3 m and 24.4 m drain spacings (except CS-4) showed better NO<sub>3</sub>-N retention and lower leaching losses than those with 12.2 m spacing (CS-1 and CS-3). Crop yield results over a 3-year period indicated that CS-2 (wider spacing plot) showed the highest productivity, with up to 13.6% higher yield compared to other plots. Furthermore, when comparing plots with the same drainage designs, CS-2 and CS-4 showed 5.1% to 2.6% higher corn yield (3-year average) compared to CS-1 and CS-3, and CS-5 and CS-6, respectively. Overall, a wider drainage system showed the capacity to export lower nutrient levels while concurrently enhancing productivity. These findings represent that optimizing tile drainage systems can effectively reduce nitrate losses while increasing crop productivity.

**Keywords:** subsurface drainage; drainage design; nitrate loss; crop productivity



**Citation:** Hwang, S.; Singh, S.; Bhattarai, R.; Jeong, H.; Cooke, R.A. Impact of Subsurface Drainage System Design on Nitrate Loss and Crop Production. *Appl. Sci.* **2024**, *14*, 10180. <https://doi.org/10.3390/app142210180>

Academic Editor: Borja Velazquez-Marti

Received: 17 September 2024

Revised: 24 October 2024

Accepted: 5 November 2024

Published: 6 November 2024



**Copyright:** © 2024 by the authors. Licensee MDPI, Basel, Switzerland. This article is an open access article distributed under the terms and conditions of the Creative Commons Attribution (CC BY) license (<https://creativecommons.org/licenses/by/4.0/>).

## 1. Introduction

Subsurface (or tile) drainage is a practical and advantageous system for enhancing crop yields by controlling planting timing, managing efficient fertilizer use, and facilitating the removal of excess seasonal water from the soil [1,2]. Because of these agronomic benefits, the subsurface drainage system is strategically applied in regions with poorly drained but highly productive soils [3,4], resulting in its widespread adoption. However, alongside its widespread use, there have also been water quality concerns regarding this functional drainage system all over the world, including the United States [5], Canada [6], Sweden [7], and the U.K. [8], among others. The primary cause of these water quality concerns lies in the fact that the subsurface drainage system may create preferential pathways for the rapid transfer of contaminated water directly from agricultural fields to water bodies [9,10]. Moreover, nitrate, being a soluble substance, can easily leach into tile-drained water without undergoing soil processes that typically reduce nitrate concentrations [11].

Subsurface drainage has adverse consequences as a major contributor to nutrient loss in the aquatic environments of the Midwestern regions of the United States. According to [12], approximately 25% of total phosphorus (P) and 52% of total nitrogen (N) delivered to the Gulf of Mexico can be attributed to the corn and soybean fields of those regions. Many researchers are also concerned that the prevalence of elevated nitrate levels has also been linked to a range of environmental issues, including hypoxia in the Gulf of Mexico [13]. In particular, ref. [12] estimated that Illinois contributes around 17% of annual nitrogen flux to the Gulf, predominantly due to the widespread adoption of subsurface drainage systems. Therefore, strategic agricultural water management practices to reduce nitrate-N transport and concentration levels through subsurface drainage systems emerge as crucial and pressing environmental objectives.

The Illinois Nutrient Loss Reduction Strategy (NLRs) calls for actions to decrease the state's nutrient loads entering the Mississippi River by 15% to 25% within the next decade [14]. While the overall conclusions are clear—that broad measures may be needed across most corn-soybean regions to meet these ambitious reduction targets—many uncertainties remain at the individual farm level. The scientific complexities of nutrient losses need to be better understood, and many farmers are being urged to alter their practices and reduce nutrient inputs without a clear understanding of how specific recommendations will affect outcomes. Given the increasing need for proactive efforts, the coming years offer a critical opportunity to engage the agricultural community in scientific projects and outreach initiatives that will ultimately determine the success of the NLRs. Among the various practices contributing to this effort, one important practice is the efficient management of subsurface drainage, including the design of these systems.

The spacing and depth of subsurface drainage systems, along with soil and field characteristics, control the amount of water drained from cropland, directly impacting nitrate-nitrogen ( $\text{NO}_3\text{-N}$  or nitrate-N) losses, crop yields, and water availability for crops. Concerning the aspect of subsurface drainage design and crop yield, ref. [15] conducted a comprehensive 6-year field study in Indiana, USA, employing tile drains spaced at intervals of 10, 20, and 30 m. Their findings reported that 20 m tile spacing maximized corn yield. Ref. [16] undertook a decade-long investigation in Indiana, USA, examining the impact of three tile spacings (5, 10, and 20 m) on corn yield. Their results indicated that corn yield was inversely correlated to tile spacing. When it comes to the results of [17] in Iowa, USA, their modeling study indicated that employing a shallower drainage system could potentially heighten water stress on crop production, thereby leading to relatively diminished yields. Nevertheless, there have still been inconsistent outcomes in terms of the relations between tile spacing and depth and crop production. We also found that the previous research was conducted on a comparatively small plot, ranging from 0.1 to 0.6 ha [15,16,18,19]. Therefore, much more research on drainage design is needed, focusing on the preparation of relatively larger-scale study plots, in order to explore the effects on tile flow and nitrogen (N) losses.

Distinct operating mechanisms of subsurface drainage systems can lead to varied hydrological processes within the soil, consequently affecting nitrogen (N) losses from a field. Based on studies investigating the impact of subsurface drainage design on nitrogen (N) losses, employing wider and shallower tile installation can result in reductions in nitrogen (N) losses [20,21]. Ref. [19] showed that wider tile spacings and shallower tile depths result in reduced nitrogen (N) losses based on long-term (1915–1996) modeling studies and field measurements in Minnesota, USA. Ref. [22] also presented similar outcomes, supported by both field-monitored data and modeling results, regarding the response of nitrogen (N) losses.

While numerous studies have examined the influence of tile depth and spacing on water quality and crop yields [23–25], a definitive consensus has remained difficult to achieve. The contrasting outcomes across various research results represent the need for a scientific consensus regarding the impact of tile depth and spacing on nutrient loss from fields and crop yields. Significantly, a comprehensive investigation that examines the trade-offs between the effects of tile depth and spacing on both nitrogen (N) losses and

corn/soybean yield in Illinois has yet to be conducted. Therefore, this study aims to bridge this knowledge gap by investigating optimal practices for harmonizing drainage depth and spacing while considering water quality and crop production goals in Illinois. The specific objectives of this study are (a) to determine the impacts of different subsurface drainage design types on nitrogen (N) losses and fertilizer use efficiencies and (b) to evaluate the potential for optimizing subsurface drainage design to mitigate N losses and enhance crop production.

## 2. Materials and Methods

### 2.1. Site Description

The study field was set up in 2017 near Church Road in Champaign County ( $40^{\circ}3'10''$ – $88^{\circ}12'41''$ ), Illinois. The study field had six hydrologically separated individual subsurface drained plots, each having an area of 2 ha (total 12 ha, with approximately a maximum width of 405 m and a height of 350 m). The predominant soil at the research site was categorized as Drummer Silty Clay Loam soil. The annual average rainfall received in the area is around 967 mm from 2003 to 2022. The six plots at the research site were installed with different tile drainage configurations (spacing and depth). The tiles installed in plots CS-1 and CS-3 were spaced at 12.2 m and a depth of 1.1 m; in CS-2 and CS-4, the spacing was 24.4 m and the depth was 1.1 m; and in CS-5 and CS-6, the spacing was 18.3 m and the depth was 0.8 m (Figure 1). CS-2 and CS-4, and CS-5 and CS-6 have the same drainage coefficient. We installed perforated PVC without a filter for the lateral tiles and double-walled, corrugated, non-perforated PVC for the main tiles.

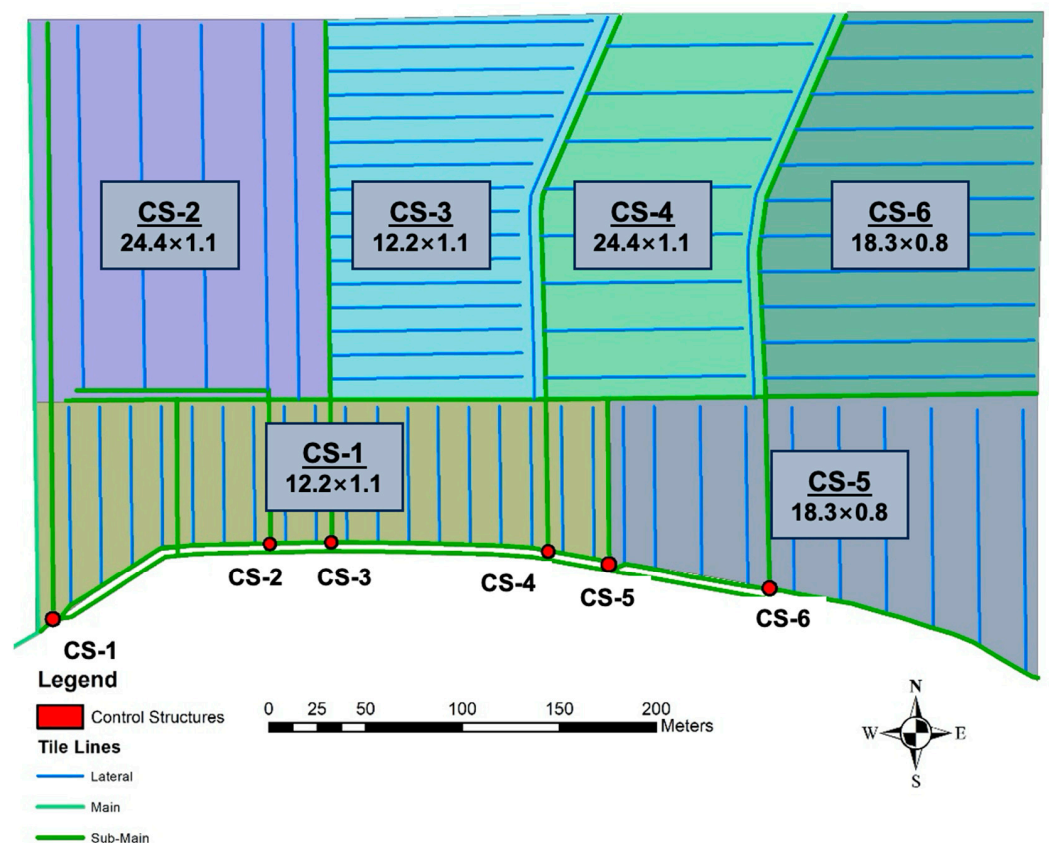


**Figure 1.** Field layout and drainage system design of CS-field.

All the CS plots were under the corn and soybean rotation system. Fertilizer in the form of urea and ammonium-nitrate solution (UAN32%) at the average rate (533 L/ha) was applied in each plot before planting corn (2019, 2020, and 2022). Additional monoammonium phosphate (MAP 11-52-0) fertilizer and potash were applied in each plot after

harvesting corn at the average rate of 2263 L/ha and 286 kg/ha, respectively. Additionally, herbicides (atrazine and rescicore) were applied before planting corn each year at the average rate of 2.8 kg/ha and 1.12 kg/ha, respectively.

## 2.2. Topographical Analysis

Our research field comprised a relatively larger scale (2 ha) of experimental plots compared to that of the other research field [15,16,18,19]. Consequently, significant differences in the Digital Elevation Model (DEM) existed, and the landscape position and land slope differences could influence tile flow. For example, certain plots may have received increased surface runoff from others due to the variations in DEM across the field. To analyze the topographical impacts on the tile flow of each plot, we utilized the Topographic Position Index (TPI) with the assistance of Lidar DEM data (Figure 2). TPI is defined as the disparity between the elevation of the central point ( $z_0$ ) and the mean elevation of its vicinity within a designated neighborhood ( $\bar{Z}$ ) [26–28].

$$TPI = Z_0 - \bar{Z}$$

Positive (+) TPI values indicate locations situated at elevations higher than the average of their surrounding areas, while negative (−) TPI values indicate locations situated at elevations lower than their surrounding areas [28]. In this study, a radius of 10 m from the target location was used to calculate the neighborhood's average elevation.

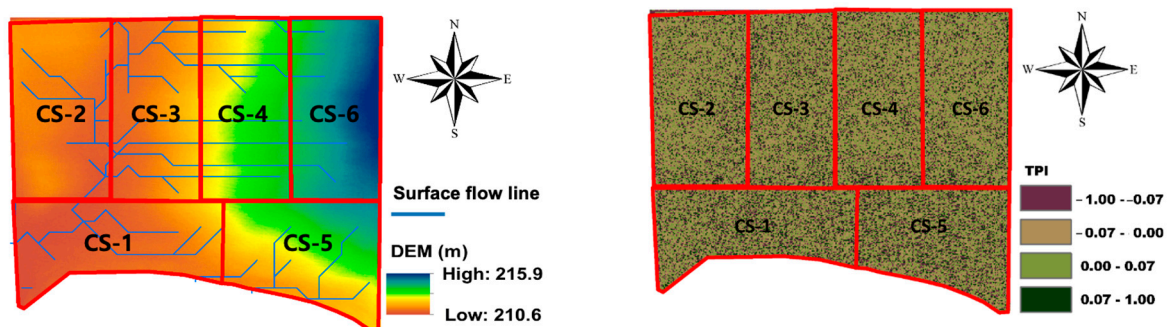


**Figure 2.** Field boundaries and surface flow line of CS-field with Lidar DEM (left) and Topographic Position Index (TPI) map (right).

The average TPI values for each field are as follows: CS-1:  $-0.0004$ , CS-2:  $0.0000$ , CS-3:  $-0.0005$ , CS-4:  $0.0003$ , CS-5:  $0.0003$ , CS-6:  $0.0010$ . According to the TPI analysis results, CS-6 was the highest position in this field, and CS-3 was the lowest position. However, when comparing the TPI median values for CS-1 and CS-3, CS-1 shows a value of  $-0.0008$ , while CS-3 shows a value of  $-0.0004$ . Therefore, if extreme values that affect the average TPI are removed, CS-1 is actually positioned lower. As shown in the DEM map, the flow lines converge toward CS-1.

## 2.3. Data Collection, System Monitoring, and Statistical Analysis

To obtain the meteorological data, we used two different data sources. The first data source was the Champaign station data, obtained from the Water and Atmospheric Resources Monitoring Program at the Illinois State Water Survey, located 4 km away from the study area. Another source of data was from field measurements collected by the WatchDog weather station near our site, located 1.6 km away. The daily meteorological data from both stations were used to validate the data and also fill in the missing values. The collected meteorological data were used to calculate the water balance for each water year from 1 October to 30 September. We also obtained the remotely sensed evapotranspiration data to calculate the water balance. We collected MODIS Evapotranspiration data (MOD16A2 product) from the NASA Distributed Active Archive Center (DAAC), which



had a 500 m spatial resolution and an 8-day data gap [29]. The product is based on the algorithm of the Penman-Monteith equation and uses the meteorological reanalysis data and 8-day remotely sensed vegetation property dynamics from MODIS to calculate 8-day evapotranspiration [29].

Each monitoring station was equipped with a v-notch weir and logger for monitoring daily drainage flow and recording water pressure at the outlet of subsurface drainage systems. The station was instrumented to measure the flow rate at 10-min intervals using a Hobo water level logger (Onset U20-001-01, Bourne, MA, USA). Two barometric sensors were installed in the control structure CS-1 and CS-6 for recording atmospheric pressure, which was used to compensate for reading errors by the individual water depth sensors at both sites.

Sensor data were downloaded once a month, and drainage flow rates were calculated using a calibrated V-notch weir equation as described by [30]. Water samples were collected twice a week (Tuesdays and Fridays) from March to October and once a week (Fridays) from November to February using the grab sampling method. Additional water samples were collected following extreme rainfall events. The collected water samples were analyzed for NO<sub>3</sub>-N in the Water Quality Laboratory of the Department of Agricultural and Biological Engineering at the University of Illinois. The samples were stored at a temperature of 4 °C until the time of analysis in the laboratory. The hydrazine sulfate reduction method with an auto-analyzer was used to determine the nitrate-N concentrations of the water samples. The detection limit for nitrate-N was 0.07 mg L<sup>-1</sup>. The measured stage and time of the recorded stages were utilized to calculate subsurface flow rates and volumes. Nitrate-N loads were calculated using nitrate-N and concentrations and computed tile flow volume based on the flow-weighted mean concentrations method. The mass loss for each plot was divided by the area of each plot and reported in kilograms per hectare (kg ha<sup>-1</sup>).

A single-factor ANOVA was performed to determine the difference in the drained water flow and nitrate-N loads and concentration, followed by Tukey's honest, significant test. A single-factor ANOVA determines whether there are statistically significant differences between the means of three or more independent groups, but it does not confirm where those differences lie. Tukey's HSD test was performed to confirm which specific group's means were different. A 95% confidence interval was adopted for both ANOVA and Tukey tests.

### 3. Results and Discussion

#### 3.1. Weather, Evapotranspiration, and Subsurface Drainage Flow

The 20-year (2003–2022) average annual precipitation in the study area was 967.4 mm yr<sup>-1</sup>. The annual precipitation records for the study period (2018–2022) show the long-term average precipitation in the year 2019 (1294.1 mm) and below-average precipitation in the year 2022 (907.8 mm). The 4-year average precipitation is 1102.8 mm yr<sup>-1</sup>. The 4-year average evapotranspiration data show 526.7 mm yr<sup>-1</sup> (Figure S1, Supplementary Material). Compared to the 4-year average precipitation data, the rate is about 47.8%.

The concept of a water year is important for considering the freezing and/or thawing effects of precipitation during the winter season [31]. Even if rainfall or snow occurs within a given year, the resulting flow may not occur until the following year due to the freezing effect. In Illinois, USA, it is more logical to include winter season precipitation from October to February within the same year. Consequently, we analyzed the monitoring data based on the water year, which spans from 15 October of the current year to October 14th of the following year.

The 4-year water precipitation, evapotranspiration, and drain water flow for each plot are summarized in Table 1. The drain flow removed an average of 41.6% of rainwater from the six plots over 4 years. The evapotranspiration rate is about 49% of the average annual precipitation. The drain water flow percentages of rainwater for the six sites (CS-1 to CS-6) were 64.3%, 34.5%, 57.6%, 38.6%, 39.1%, and 15.7%. These results are comparable and within the range (except CS-1 and CS-3) reported in other similar regional studies [20,32,33].

In a 4-year field study conducted in Iowa, ref. [32] found that the percentage distribution of total precipitation to drain water flow ranged between 18–40%. Ref. [20] reported that 8% to 20% of annual precipitation contributed to the average annual drain water flow in a 3-year field study in Indiana. In another study, ref. [5] found that drain water flow percentages of precipitation ranged from 15% to 22% in a 10-year study in Illinois. In the third year, surface runoff and percolation rates were higher than in other years due to flooding events. There were more flooding events in the third year compared to the other monitoring years. As a result, there was more surface runoff than in the second year, even though the second year had more rainfall than the third. We did not measure the runoff and percolation rates directly, which is a limitation of this research.

**Table 1.** Summary of water balance according to water year from 2018 to 2022.

Water Year	Precipitation (mm)	ET (mm)	Surface Runoff + Percolation (mm)	Subsurface Drainage Flow (mm)						
				Ave.	CS-1 (12.2 m × 1.1 m)	CS-2 (24.4 m × 1.1 m)	CS-3 (12.2 m × 1.1 m)	CS-4 (24.4 m × 1.1 m)	CS-5 (18.3 m × 0.8 m)	CS-6 (18.3 m × 0.8 m)
Year 1 (October 2018–September 2019)	1077.2	575.7 (53.4) <sup>a</sup>	93.9 (8.7)	408.5 (37.9)	697.3 (64.7)	366.5 (34.0)	607.4 (56.4)	358.6 (33.3)	274.7 (25.5)	146.4 (13.6)
Year 2 (October 2019–September 2020)	1141.5	527.7 (46.2)	57.4 (5.0)	557.6 (48.8)	754.3 (66.1)	577.3 (50.6)	744.8 (65.2)	521.6 (45.7)	479.2 (42.0)	268.2 (23.5)
Year 3 (October 2020–September 2021)	1085.3	506.4 (46.7)	210.0 (19.4)	369.6 (34.1)	720.3 (66.4)	270.6 (24.9)	450.5 (41.5)	281.6 (25.9)	389.0 (35.8)	105.5 (9.7)
Year 4 (October 2021–September 2022)	930.4	474.7 (51.0)	28.3 (3.0)	427.4 (45.9)	557.9 (60.0)	264.1 (28.4)	626.8 (67.4)	474.3 (51.0)	493.5 (53.0)	147.7 (15.9)
Average (October 2018–September 2022)	1058.6	521.1 (49.2)	97.4 (9.2)	440.1 (41.6)	682.5 (64.3)	369.6 (34.5)	607.4 (57.6)	404.9 (38.6)	409.1 (39.1)	167.0 (15.7)

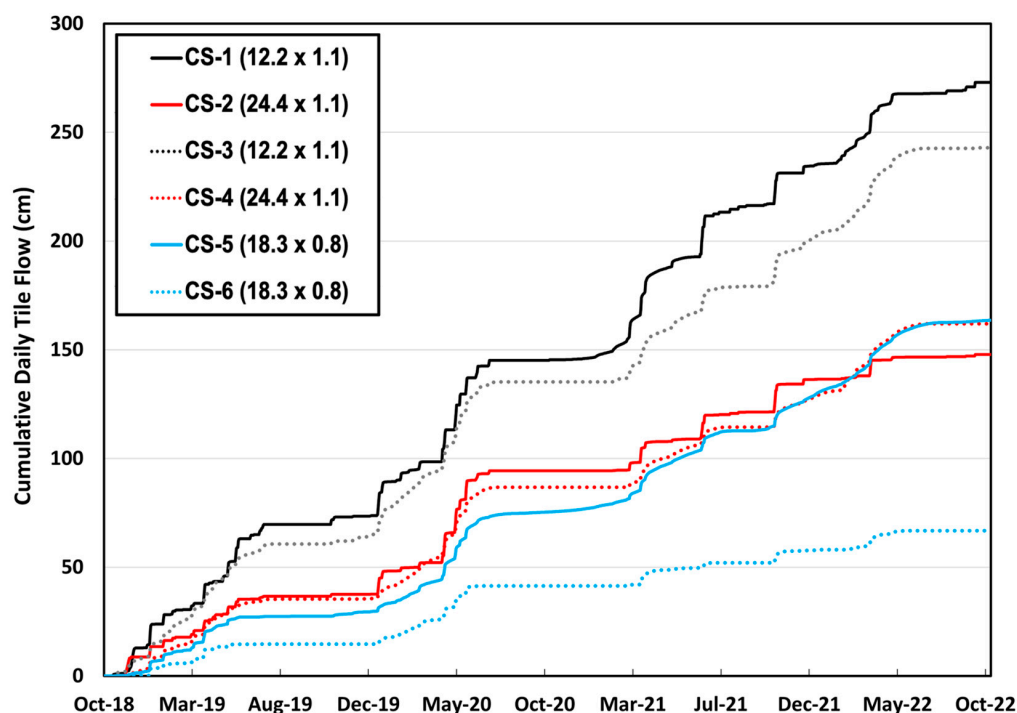
<sup>a</sup>: Ratio to precipitation (%). Data sources: Precipitation-Champaign weather station (Illinois Water survey) and observed data (WatchDog); ET-MODIS16A2 (NASA DAAC); Subsurface drainage flow: Observed data; Surface runoff + percolation: Precipitation-ET-Subsurface drainage flow. Water year: from 1 October this year to 30 September next year.

Figure 3 shows the total drain water flow observed during all plot monitoring periods. Plot CS-1 had the highest percentage of drain water flow compared to the other plots, followed by plots CS-3, CS-5, CS-4, CS-2, and CS-6. The highest total drain flow of 273.0 cm was recorded in plot CS-1, and the lowest drain flow of 66.8 cm was recorded in plot CS-6 in a 4-year field study. CS-1 and CS-3 had a higher flow rate range than observed in the referenced studies. The higher percentage of drain water flow recorded in plots CS-1 and CS-3, associated with narrow drain spacing, resulted in an accelerated drainage discharge of rainwater compared to the other plots.

Following an analysis of the topographic position index (TPI) results, a comparison of the average and median values across each field reveals that the CS-1 plot is at the lowest elevation, while CS-6 is at the highest elevation. This may contribute to surface runoff from other plots onto plot CS-1 and surface runoff loss from plot CS-6.

CS-2, CS-4, and CS-5 have the same drainage coefficient, resulting in similar tile flow results. Although CS-6 has the same drainage coefficient as these fields, it shows lower tile flow results. This disparity can also be attributed to the topographical characteristics of plot CS-6, situated at the highest elevation within the fields (Figure 2). When segmenting the study fields into the east and west parts, CS-2 is located in the highest position within the west part, whereas CS-6 is situated in the highest position within the east part. Consequently, based on the findings from the surface flow line analysis, even though the elevation of plot CS-2 is lower than that of plots CS-4, CS-5, and CS-6, its total tile flow

is slightly lower compared to the tile flow results observed in plots CS-4 and CS-5. Thus, spatial differences in topography and soil types were also reflected in these results through the TPI analysis and surface flow line results.



**Figure 3.** Cumulative daily tile flow at each site from 2018 to 2022.

Throughout the study period, we observed four growing seasons (from mid-May to mid-October) and four non-growing seasons (from mid-October to mid-May). An average annual precipitation of  $463.0 \text{ mm yr}^{-1}$  was received during the growing season, whereas, during non-growing seasons, an average annual precipitation of  $562.5 \text{ mm yr}^{-1}$  was received. Drain flow occurred sporadically throughout the growing seasons, typically at the beginning or during heavy rainfall events. During the non-growing seasons (mainly between November and January), most plots had very small tile flow due to low precipitation or frozen soil conditions (Figure S2).

The results of the precipitation and drain water flow observed during growing and non-growing seasons are presented in Table 2. During the crop growing season, the percentage of drain flow to precipitation was recorded in the range of 0.5% (CS-6) to 66.8% (CS-1). One reason why the higher percentage of drain water flow during the fourth non-growing season is associated with flooding and the backwater effect is that it causes the percentage of rainwater in the drain flow to exceed 100% (CS-3).

We conducted an ANOVA (analysis of variance) single-factor test to compare the mean daily discharge between the plots. The analysis results showed that one or more plots have a significantly different mean daily discharge, with a  $p$ -value of  $2 \times 10^{-16}$  at a 95% confidence interval ( $p < 0.05$ ). Among the various ANOVA test methods, we used Tukey's HSD test to identify which plot group has a significantly different mean discharge of daily flow. The Tukey's test results in Figure 4 indicate that the mean drainage discharge in plots CS-1 and CS-3 significantly differs from that of CS-2, CS-4, CS-5, and CS-6 ( $p < 0.05$ ).

Additionally, there is no significant difference in flow observed among plots CS-2, CS-4, and CS-5. However, plot CS-6 shows significant differences from all other fields. This result also draws a very similar conclusion to the total flow analysis. The result suggests that plots with narrower drain spacing have higher mean discharge than plots with wider drain spacing.

**Table 2.** Summary of precipitation and subsurface flow during growing and non-growing seasons from 2018 to 2022.

Seasons	Rainfall (mm)	Subsurface Drainage Flow (mm) (Subsurface Flow as a Percentage of Rainfall, %)						Ave.
		CS-1 (12.2 m × 1.1 m)	CS-2 (24.4 m × 1.1 m)	CS-3 (12.2 m × 1.1 m)	CS-4 (24.4 m × 1.1 m)	CS-5 (18.3 m × 0.8 m)	CS-6 (18.3 m × 0.8 m)	
N-G <sup>a</sup> Season 1	694.9	526.6 (75.8)	317.5 (45.7)	501.1 (72.1)	315.3 (45.4)	260.5 (37.5)	144.7 (20.8)	344.3 (49.5)
G <sup>b</sup> Season 1	382.3	170.8 (44.7)	49.0 (12.8)	106.2 (27.8)	43.3 (11.3)	14.2 (3.7)	1.8 (0.5)	64.2 (16.8)
N-G Season 2	662.9	434.7 (65.6)	293.2 (44.2)	467.5 (70.5)	303.3 (45.8)	263.6 (39.8)	170.7 (25.7)	322.2 (48.6)
G Season 2	478.5	319.6 (66.8)	284.2 (59.4)	277.3 (58.0)	218.3 (45.6)	215.6 (45.1)	97.5 (20.4)	235.4 (49.2)
N-G Season 3	468.9	461.5 (98.4)	143.1 (30.5)	276.8 (59.0)	160.8 (34.3)	241.0 (51.4)	77.6 (16.5)	226.8 (48.4)
G Season 3	616.5	258.9 (42.0)	127.5 (20.7)	173.7 (28.2)	120.8 (19.6)	147.9 (24.0)	27.9 (4.5)	142.8 (23.2)
N-G Season 4	555.8	505.5 (90.9)	251.2 (45.2)	586.7 (105.6)	437.7 (78.8)	428.0 (77.0)	145.4 (26.2)	392.4 (70.6)
G Season 4	374.7	52.4 (14.0)	12.9 (3.4)	40.1 (10.7)	36.6 (9.8)	65.5 (17.5)	2.3 (0.6)	35.0 (9.3)
N-G Season Ave.	562.5	467.2 (83.1)	229.2 (40.7)	443.6 (78.9)	298.4 (53.0)	310.9 (55.3)	131.2 (23.3)	313.4 (55.7)
G Season Ave.	463.0	200.4 (43.3)	118.4 (25.6)	149.4 (32.3)	103.4 (22.3)	110.8 (23.9)	32.4 (7.0)	119.1 (25.7)

<sup>a</sup>: non-growing, <sup>b</sup>: growing.

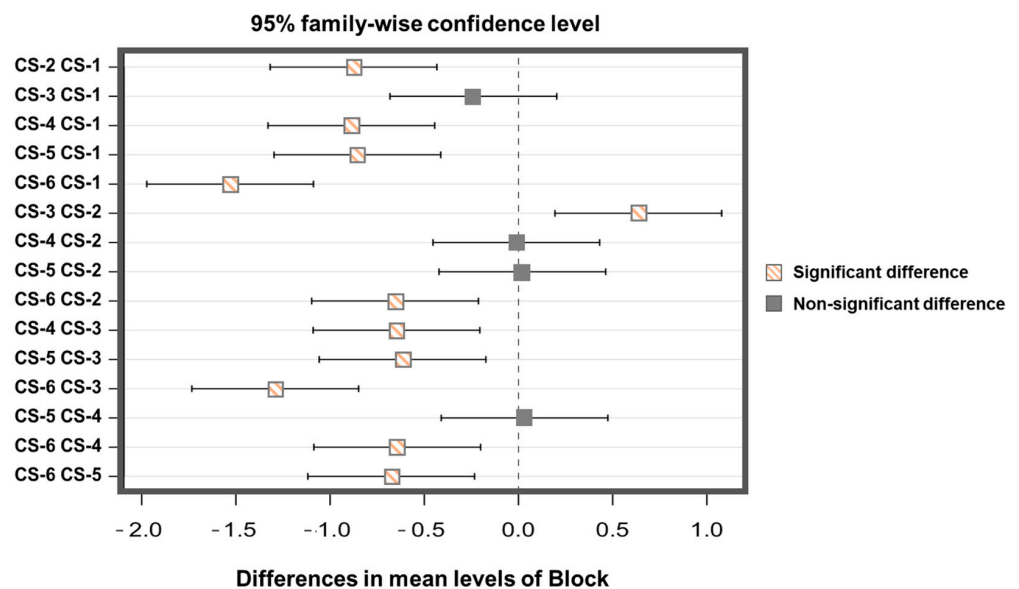


**Figure 4.** Drainage flow differences between plots were analyzed using Tukey’s test ( $p < 0.05$ ). CS-1 and CS-4, and CS-2, CS-4, and CS-5 showed no significant differences.

The daily nitrate-nitrogen ( $\text{NO}_3\text{-N}$ ) load ( $\text{kg N ha}^{-1}$ ),  $\text{NO}_3\text{-N}$  concentration ( $\text{mg L}^{-1}$ ), and mean  $\text{NO}_3\text{-N}$  concentration for all six plots from 2018 to 2022 are presented in Figure S3. The  $\text{NO}_3\text{-N}$  concentration in subsurface water samples fluctuated from almost zero to



73.6 mg L<sup>-1</sup> for sites CS-1 to CS-6. During the study period, the highest mean NO<sub>3</sub>-N concentration of 20.3 mg L<sup>-1</sup> was observed in plot CS-6, and the minimum mean NO<sub>3</sub>-N concentration of 7.5 mg L<sup>-1</sup> was observed in plot CS-2. In CS-1 and CS-2, the daily NO<sub>3</sub>-N concentration in drainage flows was below USEPA's drinking water standard of 10 mg L<sup>-1</sup> most of the time (Figure S3). However, the NO<sub>3</sub>-N concentration in drain flow from plots CS-3, CS-4, CS-5, and CS-6 often exceeded the USEPA's limit (10 mg L<sup>-1</sup>). The concentration of NO<sub>3</sub>-N in the drain flow in each plot varied widely from month to month. Peak concentration was observed at the beginning of the corn planting season (mainly in May each year) and late fall after harvesting the crops. This variation in the NO<sub>3</sub>-N is associated with pre-planting and late fall N applications.

For annual nitrate loss, plot CS-3 had the highest loss compared to other plots (Table 3). Even though CS-1 had higher tile flow compared to CS-3, CS-3 had relatively higher tile flow and nitrate concentration from 2018 to 2020. Another noteworthy observation is that CS-4 shows greater total nitrate loss compared to CS-1. According to Figure S3, CS-4 kept higher levels of NO<sub>3</sub>-N effluent concentration spanning from 2018 to the middle of 2020. Consequently, despite the comparatively less volume of water flow from the field within the confines of CS-4, in comparison to the drainage plots of CS-1 designed by narrower drain spacing, the amount of nitrate loss, as quantified by the product of water volume and effluent concentration, had a substantial result.

**Table 3.** Yearly nitrate-N loss (kg/ha) at each site from 2018 to 2022.

Year	CS-1 (12.2 m × 1.1 m)	CS-2 (24.4 m × 1.1 m)	CS-3 (12.2 m × 1.1 m)	CS-4 (24.4 m × 1.1 m)	CS-5 (18.3 m × 0.8 m)	CS-6 (18.3 m × 0.8 m)	Ave.
Year 1 (October 2018–September 2019)	67.2	31.4	85.4	82.8	47.3	32.0	57.7
Year 2 (October 2019–September 2020)	76.7	62.7	98.2	79.0	76.8	45.8	73.2
Year 3 (October 2020–September 2021)	38.6	15.3	29.0	13.6	38.5	21.1	26.0
Year 4 (October 2021–September 2022)	49.0	17.6	65.7	67.5	42.0	17.1	43.1
Ave. (October 2018–September 2022)	57.9	31.7	69.6	60.7	51.1	29.0	50.0

Upon conducting a comparative analysis of the outcomes over various years, it was found that Year 2, characterized by higher precipitation levels (the wettest year), showed the most pronounced NO<sub>3</sub>-N loss. Year 3, not Year 4, which had the least rainfall, showed the lowest nitrogen loss. This result can be attributed to the fact that, in Year 3, soybeans were cultivated and there was a relatively reduced use of fertilizers. This trend is further supported by the data in Figure S3, which show that the nitrogen effluent concentrations from each plot in Year 3 were lower compared to the years with corn cultivation. Thus, when exclusively considering the variables of rainfall and corn cultivation, it becomes evident that the nitrogen loss during Year 4, which had the least amount of rainfall, was actually the lowest among the corn cultivation years.

We extended the approach to calculating the cumulative NO<sub>3</sub>-N loads for each plot (Figure 5). Over the study period, we observed total NO<sub>3</sub>-N losses ranging from 116.0 to 278.3 kg N ha<sup>-1</sup> for all plots (CS-1: 164.3, CS-2: 127.0, CS-3: 278.3, CS-4: 242.9, CS-5: 204.6, and CS-6: 116.0 kg N ha<sup>-1</sup>). We found that plots with wider drain spacing of 18.3 m and 24.4 m (except CS-4) had fewer NO<sub>3</sub>-N losses (range 116.0 to 204.6 kg N ha<sup>-1</sup>) compared to plots with 12.2 m drain spacing (164.3 and 278.3 kg N ha<sup>-1</sup>). The plots with wider drain spacing had less drain flow, due to which soil retained more NO<sub>3</sub>-N.

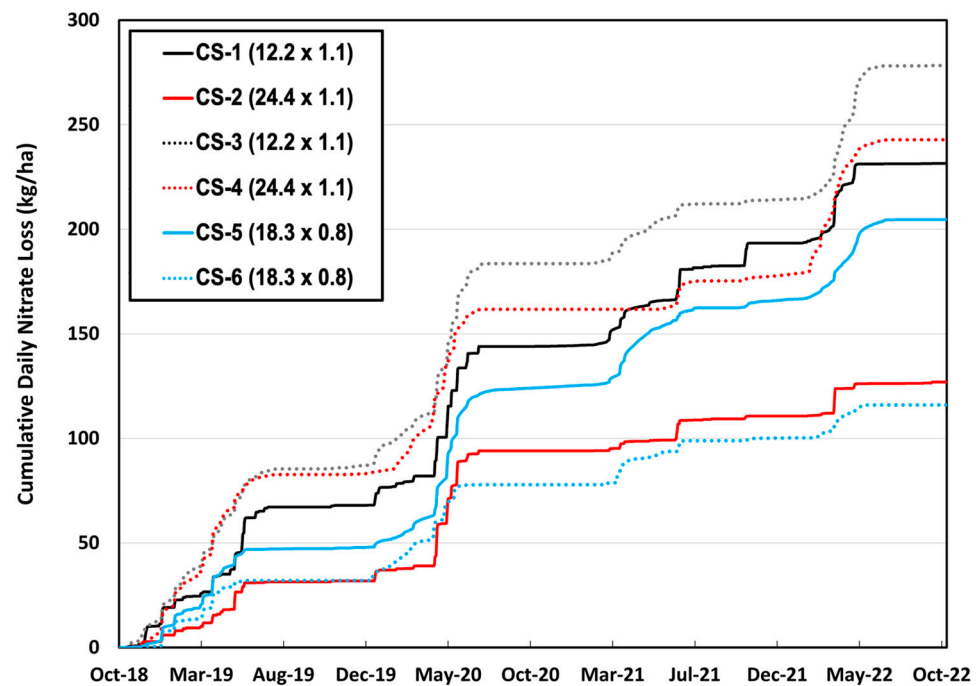


Figure 5. Cumulative daily nitrate-N loss at each site from 2018 to 2022.

In plot CS-4, we observed relatively higher  $\text{NO}_3\text{-N}$  losses compared to CS-2 and CS-5, which are set up with the same drainage coefficient, despite showing similar total cumulative tile flow. This is due to the consistently higher nitrate concentrations in CS-4, while CS-2 showed lower concentrations at the beginning of the monitoring years (Figure S3). These differences may be attributed to the complex interaction of nitrate loss with factors such as temperature, soil moisture, soil microbial activity, snowmelt, soil types, etc.

The observation also showed that the  $\text{NO}_3\text{-N}$  load was higher in drainage water during the non-growing season compared to the growing season. This is apparently because most tile flow occurs during the non-growing season. The average load during the non-growing season ranged from  $16.5 \text{ kg N ha}^{-1}$  to  $42.3 \text{ kg N ha}^{-1}$ , whereas during the growing season, the average load ranged from  $4.8 \text{ kg N ha}^{-1}$  to  $20.7 \text{ kg N ha}^{-1}$  (Table 4).

Table 4. Nitrate-N (kg/ha) load in drain flow during growing and non-growing seasons (2018–2022).

Seasons	CS-1 (12.2 m × 1.1 m)	CS-2 (24.4 m × 1.1 m)	CS-3 (12.2 m × 1.1 m)	CS-4 (24.4 m × 1.1 m)	CS-5 (18.3 m × 0.8 m)	CS-6 (18.3 m × 0.8 m)	Ave.
N-G Season 1	45.4	26.5	71.1	73.3	44.2	31.5	292.0
G Season 1	21.8	4.9	14.3	9.4	3.1	0.5	54.0
N-G Season 2	33.4	27.9	48.7	51.6	33.6	35.6	230.8
G Season 2	43.3	34.7	49.5	27.4	43.2	10.2	208.3
N-G Season 3	21.5	4.9	18.9	0.0	28.0	13.4	86.8
G Season 3	17.2	10.3	10.1	13.6	10.4	7.6	69.2
N-G Season 4	48.7	16.8	59.3	63.5	35.9	16.1	240.3
G Season 4	0.3	0.8	6.4	4.0	6.1	1.0	18.6
N-G Season Ave.	34.5	16.5	42.3	38.4	32.5	21.7	186.0
G Season Ave.	20.7	12.7	20.1	13.6	15.7	4.8	87.5

We also performed Tukey's test to identify whether the plots' mean  $\text{NO}_3\text{-N}$  load in drainage water differs and if the spacing and depth influence the  $\text{NO}_3\text{-N}$  load. The mean  $\text{NO}_3\text{-N}$  load was non-significantly different between plots CS-1 and CS-3, CS-1 and CS-4, CS-1 and CS-5, CS-2 and CS-5, CS-2 and CS-6, CS-3 and CS-4, and CS-4 and CS-5 (Figure 6). The Tukey's test showed that the mean  $\text{NO}_3\text{-N}$  losses ( $\text{kg N ha}^{-1}$ ) from plots with wider drain spacing significantly differed from plots with narrow drain spacing. The one exception that we observed was between plots CS-2 and CS-4. Both plots had the same drain spacing and depth, but the mean  $\text{NO}_3\text{-N}$  load differed significantly. This may be attributed to surface runoff from plot CS-6 to plot CS-4 during peak rainfall events, contributing to higher nutrient deposition.

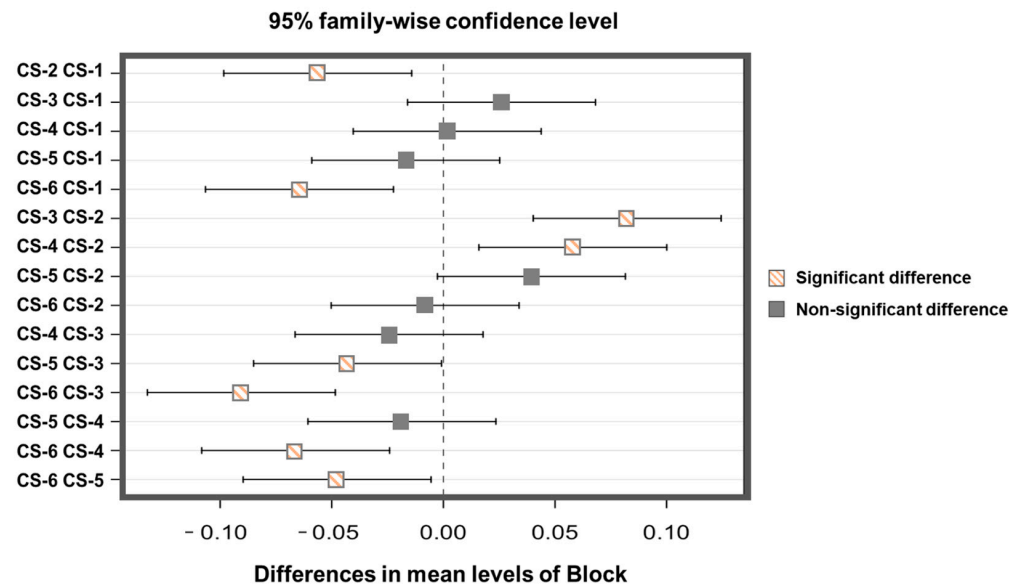


**Figure 6.**  $\text{NO}_3\text{-N}$  load differences between plots were analyzed using Tukey's test ( $p < 0.05$ ). CS-1, CS-3, and CS-4 and CS-1 and CS-5, CS-2 and CS-5 and CS-2 and CS-6 showed no significant differences.

### 3.2. Soil Nitrate Concentration for Each Plot

This study was conducted to establish the relationships between subsurface drainage design and the exported water quality from each plot. If there was a significant variation in nitrate concentrations within each plot's soil due to nitrate treatments, this imbalance could potentially affect the initial research findings we aimed to determine. To resolve this issue, we conducted soil samplings prior to sowing in both 2021 and 2022, following the NRCS soil sampling procedure for nutrient management. For soil sampling, we collected two composite soil samples from each plot at depths of 0–15 cm (shallow soil layer) and 15–30 cm (deep soil layer). This process involved collecting 20 equal-sized soil core samples in a random pattern across each plot for each sampling depth. The 20 soil cores collected for each sampling depth were then thoroughly composited into a single representative sample for each plot. Figure 7 presents the soil nitrate concentrations for each plot in both 2021 and 2022. The findings indicate that nitrate concentrations ranged from 2.9 to 8.8 ppm in the surface layer and from 4.6 to 6.4 ppm in the subsurface layer over the 2-year period. Averaging nitrate concentrations revealed a slightly higher concentration (5.4 ppm) in the shallower depth (0–15 cm) compared to the deeper depth (15–30 cm), with an overall soil concentration of 5.2 ppm across the entire field. Additionally, the observations indicated that nitrate concentration variability in the soil was slightly greater at the shallower depth than at the deeper depth across the plots. As a result, the nitrate concentration in the soil exhibits minimal variation between depths and years across the plots.

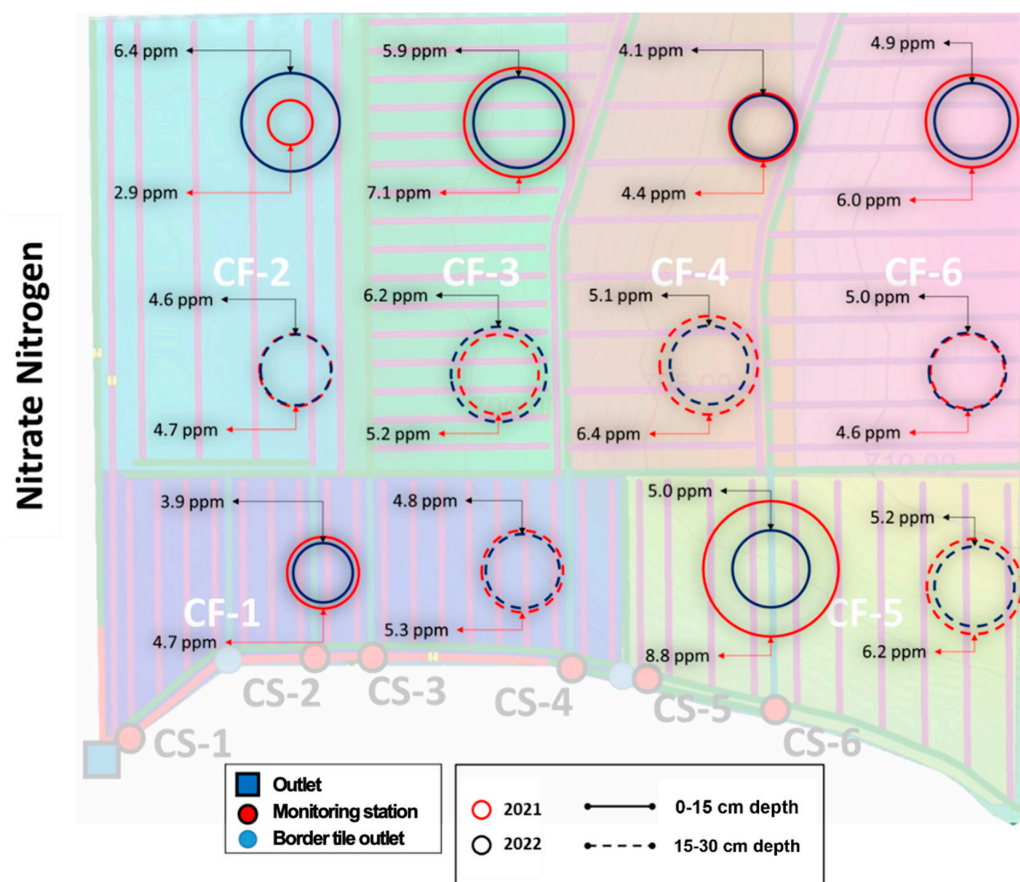


**Figure 7.** Nitrate concentration of soil below 0–15 cm and 15–30 cm. The nitrate concentration in the soil exhibits variation between depths and years across the plots.

### 3.3. Crop Yield Response

Crop yield in each plot was mapped during harvesting using a yield mapping monitor mounted on the grain combine harvester. The harvester recorded information such as grain flow, moisture, area covered, and location. Crop yield data were recorded in 2018, 2020, 2021, and 2022 for each plot. However, due to technical issues with the combine harvester's yield mapping system, the crop yield data for 2019 were lost. Table 5 shows the average annual yield for each plot in 2018, 2020, 2021, and 2022. We observed a consistent crop yield pattern across the plots during the recorded years. The soybean yield followed a similar trend to the corn yield in 2021. On average, plots with the same design combination, CS-2 and CS-4, showed a 5.1% to 2.6% higher corn yield (3-year average) compared to CS-1 and CS-3, and CS-5 and CS-6, respectively. Among the individual plots, the highest average corn yield recorded was  $11,332 \text{ kg ha}^{-1}$  in CS-2, followed by CS-3, CS-6, CS-4, and CS-5. The lowest average corn yield recorded was  $9976 \text{ kg ha}^{-1}$  in CS-1. We observed a substantial difference in corn yield between the plots with different drainage spacing and depth.

Our particular interest lay in the observations regarding drainage design, nitrate losses, and productivity within the CS-2 plot. The results observed in the CS-2 plot showed relatively lower tile flow and nitrate loss while also demonstrating the highest corn productivity, despite having a wider drainage design. These findings differ from those reported in previous research studies [25,34]. Generally, subsurface drainage systems with a narrower design are more effective at controlling excess water than wider systems. Previous research on yield results suggests that narrower subsurface drainage positively affects productivity. From the overall results of our observations, we can infer that corn and soybean plants in CS-2 utilized more water and nitrate from the soil. The higher water

retention in the soil also influences longer microbial processes facilitated by saturated water, which may have contributed to the higher crop yield observed in the CS-2 plot compared to other plots. Therefore, we suggest optimizing the drainage design with a correctly wider and deeper system to enhance productivity while pursuing sustainability by reducing nutrient loss for the environment.

**Table 5.** Crop yield (wet weight, kg/ha) in plots CS-1 to CS-6 (2018, 2020, 2021 and 2022).

Year	Crop	CS-1 (12.2 m × 1.1 m)	CS-2 (24.4 m × 1.1 m)	CS-3 (12.2 m × 1.1 m)	CS-4 (24.4 m × 1.1 m)	CS-5 (18.3 m × 0.8 m)	CS-6 (18.3 m × 0.8 m)	Ave.
2018	Corn	10,139 ± 2565	10,660 ± 2900	10,825 ± 1394	10,962 ± 2020	10,686 ± 2662	10,892 ± 2978	10,694 ± 130
2020	Corn	7904 ± 3466	11,335 ± 3354	10,646 ± 898	10,492 ± 1305	9282 ± 3200	10,816 ± 2970	10,079 ± 758
2021	Soybean	4649 ± 2114	5432 ± 1302	4895 ± 1419	4754 ± 1181	4831 ± 1628	4886 ± 1275	4908 ± 270
2022	Corn	11,885 ± 2657	12,001 ± 2233	12,416 ± 1930	11,643 ± 1653	11,836 ± 2024	11,903 ± 1902	11,947 ± 287
3 years Ave.	Corn	9976 ± 1995	11,332 ± 671	11,296 ± 974	11,032 ± 579	10,601 ± 1279	11,204 ± 607	10,907 ± 952

#### 4. Conclusions

Subsurface drainage has demonstrated its capacity to enhance the productivity of poorly drained soils; however, it concurrently increases nutrient leaching through the soil profile. Our 4-year investigation indicated that tile drainage configuration significantly influences drain flow and nutrient losses. Comparisons between narrowly spaced and widely spaced tile-drained plots revealed significant variations in drain flow, with tile drains removing an average of 41.6% of rainwater across the six plots. We found that plots with a drain spacing of 24.4 m (CS-2 and CS-4) and a drain spacing of 18.3 m (CS-5 and CS-6) showed 40% and 55% lower drain flows, respectively, compared to plots with a drain spacing of 12.2 m (CS-1 and CS-3). This suggests that the narrower drain spacing in the plots has a significant influence on drain flow. Seasonal tile flow showed that the non-growing season accounted for approximately three times more flow than the crop-growing season across all plots. During the growing season, drainage flow ranged between 32 mm and 201 mm (removing an average of 25.7% of rainwater), while in the non-growing season it ranged from 131 mm to 468 mm (removing an average of 55.7% of rainwater). On average, for each plot, total tile flow over the 4 years during the non-growing season was 94% (CS-2) to 305% (CS-6) higher than during the crop-growing season.

The mean  $\text{NO}_3\text{-N}$  concentration in drainage water was higher than  $10 \text{ mg L}^{-1}$  in most plots, except for CS-1 and CS-2. Our field records showed that plots with wider drain spacing retained more  $\text{NO}_3\text{-N}$  than those with narrower spacing and deeper drains, except for CS-4. The average annual  $\text{NO}_3\text{-N}$  losses from all plots over 4 years were around  $50 \text{ kg N ha}^{-1}$ . Cumulative 4-year  $\text{NO}_3\text{-N}$  losses from plots CS-2 and CS-4 (24.4 m drain spacing) and CS-5 and CS-6 (18.3 m drain spacing) were 27% and 37% lower, respectively, compared to CS-1 and CS-3 (12.2 m drain spacing). Plot CS-4 showed  $\text{NO}_3\text{-N}$  losses that were 77%, 16%, and 99% higher compared to CS-2, CS-5, and CS-6, respectively, despite four plots having the same drainage coefficient properties. Our observations indicated that tile flow results are highly influenced by physical variables such as drainage design, drainage coefficient, soil types, landscape position, and land slope. However, when considering water quality from agricultural fields, the mechanism is influenced not only by physical variables but also by biochemical effects in the soil. Therefore, it is evident that  $\text{NO}_3\text{-N}$  losses are influenced by various factors beyond drainage design alone. Seasonal  $\text{NO}_3\text{-N}$  losses showed that the non-growing season accounted for approximately twice the  $\text{NO}_3\text{-N}$



losses of the crop-growing season across all plots. On average, for each plot, 4-year NO<sub>3</sub>-N losses during the non-growing season were 30% (CS-2) to 352% (CS-6) higher than those during the crop-growing season.

Corn yield data from 2018, 2020, and 2022 showed higher yields in plot CS-2, followed by CS-3, CS-6, CS-4, CS-5, and CS-1. CS-2 showed relatively less NO<sub>3</sub>-N loss with higher tile flow compared to CS-6, resulting in higher productivity than the other fields. Consequently, the comprehensive analysis suggests that a wider drainage system could potentially reduce nitrate losses and promote sustainability for both the environment and agricultural productivity. However, in fields with wider subsurface drainage, there is a risk of temporarily discharging nitrate nitrogen at high concentrations during drainage events due to the accumulation of nitrate nitrogen in the soil that cannot be drained. Therefore, to mitigate the limitations associated with subsurface drainage design, agricultural engineering measures such as actively controlling the subsurface water table or implementing additional facilities (e.g., bioreactors) seem necessary.

This study highlights the substantial influence of subsurface drainage design on drain flow, nutrient losses, and crop yield, with potential for optimization to enhance crop productivity and reduce nutrient losses. However, it is clear that measures to address the inherent field uncertainty in the current research should also be considered. Specifically, further research and extended field observations—such as soil profiling, hydraulic conductivity, soil water retention curves, infiltration rates, water table fluctuations, and changes in soil moisture over time—will provide deeper insights into the outcomes of this field study. We will also consider a modeling study on how the drainage design influences hydrology and crop yield to reach a comprehensive conclusion based on various scenarios using this valuable monitoring study.

**Supplementary Materials:** The following supporting information can be downloaded at: <https://www.mdpi.com/article/10.3390/app142210180/s1>, Figure S1: 8-day evapotranspiration from 2018 to 2022 (MOIDS16A2). Figure S2: Daily drainage discharge and daily precipitation at each site from 2018 to 2022. Figure S3: Daily Nitrate-N concentrations and loss for each plot from 2018–2022.

**Author Contributions:** Conceptualization, H.J., R.A.C. and R.B.; methodology, H.J., R.A.C. and R.B.; formal analysis, S.S. and S.H.; resources, R.A.C. and R.B.; data curation, H.J., S.S. and S.H.; writing—original draft preparation, S.S. and S.H.; writing—review and editing, S.H. and R.B.; visualization, S.S. and S.H.; supervision, R.B.; project administration, R.A.C. and R.B.; funding acquisition, R.A.C. and R.B. All authors have read and agreed to the published version of the manuscript.

**Funding:** This study was supported by the Illinois Nutrient Research & Education Council (project # 2018-3-360624-356). A partial support was provided by the National Institute of Food and Agriculture, U.S. Department of Agriculture, Hatch project (No. ILLU-741-337). This work was supported by the National Research Foundation of Korea Grant funded by the Korean Government (NRF-RS-2023-00250791).

**Institutional Review Board Statement:** Not applicable.

**Informed Consent Statement:** Not applicable.

**Data Availability Statement:** The raw data supporting the conclusions of this article will be made available by the authors on request.

**Conflicts of Interest:** The authors declare no conflict of interest.

## References

1. Fausey, N.R. Drainage management for humid regions. *Int. Agric. Eng. J.* **2005**, *14*, 209–214.
2. Cooke, R.; Verma, S. Performance of drainage water management systems in Illinois, United States. *J. Soil Water Conserv.* **2012**, *67*, 453–464. [[CrossRef](#)]
3. Zucker, L.A.; Brown, L.C. *Agricultural Drainage: Water Quality Impacts and Subsurface Drainage Studies in the Midwest*; University of Minnesota Extension: St Paul, MN, USA, 1988.
4. Nangia, V.; Gowda, P.H.; Mulla, D.J.; Sands, G.R. Modeling Impacts of Tile Drain Spacing and Depth on Nitrate-Nitrogen Losses. *Vadose Zone J.* **2010**, *9*, 61–72. [[CrossRef](#)]

5. Kalita, P.K.; Cooke RA, C.; Anderson, S.M.; Hirschi, M.C.; Mitchell, J.K. Subsurface Drainage and Water Quality: The Illinois Experience. *Trans. ASABE* **2007**, *50*, 1651–1656. [[CrossRef](#)]
6. Sunohara, M.D.; Craiovan, E.; Topp, E.; Gottschall, N.; Drury, C.F.; Lapen, D.R. Comprehensive Nitrogen Budgets for Controlled Tile Drainage Fields in Eastern Ontario, Canada. *J. Environ. Qual.* **2014**, *43*, 617–630. [[CrossRef](#)] [[PubMed](#)]
7. Stenberg, M.; Ulén, B.; Söderström, M.; Roland, B.; Delin, K.; Helander, C.-A. Tile drain losses of nitrogen and phosphorus from fields under integrated and organic crop rotations. A four-year study on a clay soil in southwest Sweden. *Sci. Total Environ.* **2012**, *434*, 79–89. [[CrossRef](#)] [[PubMed](#)]
8. Edwards, A.C.; Withers PJ, A. Transport and delivery of suspended solids, nitrogen and phosphorus from various sources to freshwaters in the UK. *J. Hydrol.* **2008**, *350*, 144–153. [[CrossRef](#)]
9. Fausey, N.R.; Brown, L.C.; Belcher, H.W.; Kanwar, R.S. Drainage and Water Quality in Great Lakes and Cornbelt States. *J. Irrig. Drain. Eng.* **1995**, *121*, 283–288. [[CrossRef](#)]
10. Köhne, S.; Lennartz, B.; Köhne, J.M.; Šimůnek, J. Bromide transport at a tile-drained field site: Experiment, and one- and two-dimensional equilibrium and non-equilibrium numerical modeling. *J. Hydrol.* **2006**, *321*, 390–408. [[CrossRef](#)]
11. Poole, C.A.; Skaggs, R.W.; Youssef, M.A.; Chescheir, G.M.; Crozier, C.R. Effect of Drainage Water Management on Nitrate Nitrogen Loss to Tile Drains in North Carolina. *Trans. ASABE* **2018**, *61*, 233–244. [[CrossRef](#)]
12. Alexander, R.B.; Smith, R.A.; Schwarz, G.E.; Boyer, E.W.; Nolan, J.V.; Brakebill, J.W. Differences in Phosphorus and Nitrogen Delivery to The Gulf of Mexico from the Mississippi River Basin. *Environ. Sci. Technol.* **2008**, *42*, 822–830. [[CrossRef](#)] [[PubMed](#)]
13. Rabalais, N.N.; Turner, R.E.; Wiseman, W.J., Jr. Gulf of Mexico hypoxia, aka “The dead zone”. *Annu. Rev. Ecol. Syst.* **2002**, *33*, 235–263. [[CrossRef](#)]
14. Illinois Environmental Protection Agency. Illinois Nutrient Loss Reduction Strategy. 2024. Available online: <https://epa.illinois.gov/topics/water-quality/watershed-management/excess-nutrients/nutrient-loss-reduction-strategy.html> (accessed on 4 November 2024).
15. Hofmann, B.S.; Brouder, S.M.; Turco, R.F. Tile spacing impacts on *Zea mays* L. yield and drainage water nitrate load. *Ecol. Eng.* **2004**, *23*, 251–267. [[CrossRef](#)]
16. Kladivko, E.J.; Willoughby, G.L.; Santini, J.B. Corn Growth and Yield Response to Subsurface Drain Spacing on Clermont Silt Loam Soil. *Agron. J.* **2005**, *97*, 1419–1428. [[CrossRef](#)]
17. Singh, R.; Helmers, M.J.; Crumpton, W.G.; Lemke, D.W. Predicting effects of drainage water management in Iowa’s subsurface drained landscapes. *Agric. Water Manag.* **2007**, *92*, 162–170. [[CrossRef](#)]
18. Randall, G.W.; Huggins, D.R.; Russelle, M.P.; Fuchs, D.J.; Nelson, W.W.; Anderson, J.L. Nitrate losses through subsurface tile drainage in conservation reserve program, alfalfa, and row crop systems. *J. Environ. Qual.* **1997**, *26*, 1240–1247. [[CrossRef](#)]
19. Davis, D.M.; Gowda, P.H.; Mulla, D.J.; Randall, G.W. Modeling Nitrate Nitrogen Leaching in Response to Nitrogen Fertilizer Rate and Tile Drain Depth or Spacing for Southern Minnesota, USA. *J. Environ. Qual.* **2000**, *29*, 1568–1581. [[CrossRef](#)]
20. Kladivko, E.J.; Frankenberger, J.R.; Jaynes, D.B.; Meek, D.W.; Jenkinson, B.J.; Fausey, N.R. Nitrate Leaching to Subsurface Drains as Affected by Drain Spacing and Changes in Crop Production System. *J. Environ. Qual.* **2004**, *33*, 1803–1813. [[CrossRef](#)]
21. Sands, G.R.; Song, I.; Busman, L.M.; Hansen, B.J. The Effects of Subsurface Drainage Depth and Intensity on Nitrate Loads in the Northern Cornbelt. *Trans. ASABE* **2008**, *51*, 937–946. [[CrossRef](#)]
22. Moriasi, D.N.; Gowda, P.H.; Arnold, J.G.; Mulla, D.J.; Ale, S.; Steiner, J.L. Modeling the impact of nitrogen fertilizer application and tile drain configuration on nitrate leaching using SWAT. *Agric. Water Manag.* **2013**, *130*, 36–43. [[CrossRef](#)]
23. Kladivko, E.J.; Grochulska, J.; Turco, R.F.; Van Scoyoc, G.E.; Eigel, J.D. Pesticide and Nitrate Transport into Subsurface Tile Drains of Different Spacings. *J. Environ. Qual.* **1999**, *28*, 997–1004. [[CrossRef](#)]
24. Skaggs, R.W.; Youssef, M.A.; Chescheir, G.M.; Gilliam, J.W. Effect of drainage intensity on nitrogen losses from drained lands. *Trans. ASAE* **2005**, *48*, 2169–2177. [[CrossRef](#)]
25. Wang, X.; Mosley, C.T.; Frankenberger, J.R.; Kladivko, E.J. Subsurface drain flow and crop yield predictions for different drain spacings using DRAINMOD. *Agric. Water Manag.* **2006**, *79*, 113–136. [[CrossRef](#)]
26. Weiss, A. Topographic Position and Landforms Analysis. In Proceedings of the Poster Presentation, ESRI User Conference, San Diego, CA, USA, 9–13 July 2001; p. 200.
27. De Reu, J.; Bourgeois, J.; Bats, M.; Zwertvaegher, A.; Gelorini, V.; De Smedt, P.; Chu, W.; Antrop, M.; De Maeyer, P.; Finke, P.; et al. Application of the topographic position index to heterogeneous landscapes. *Geomorphology* **2013**, *186*, 39–49. [[CrossRef](#)]
28. Mieza, M.S.; Cravero, W.R.; Kovac, F.D.; Bargiano, P.G. Delineation of site-specific management units for operational applications using the topographic position index in La Pampa, Argentina. *Comput. Electron. Agric.* **2016**, *127*, 158–167. [[CrossRef](#)]
29. Running, S.; Mu, Q.; Zhao, M. MYD16A2 MODIS/Aqua Net Evapotranspiration 8-Day L4 Global 500 m SIN Grid V006 [Data set]. NASA EOSDIS Land Processes DAAC. 2017. Available online: <https://lpdaac.usgs.gov/products/myd16a2v006/> (accessed on 1 November 2022).
30. Chun, J.A.; Cooke, R.A. Technical Note: Calibrating Agridrain Water Level Control Structures Using Generalized Weir and Orifice Equations. *Appl. Eng. Agric.* **2008**, *24*, 595–602. [[CrossRef](#)]
31. USGS. Streamflow—Water Year 2022. 2022. Available online: <https://waterwatch.usgs.gov/2022summary/> (accessed on 6 March 2024).
32. Jaynes, D.B.; Colvin, T.S.; Karlen, D.L.; Cambardella, C.A.; Meek, D.W. Nitrate Loss in Subsurface Drainage as Affected by Nitrogen Fertilizer Rate. *J. Environ. Qual.* **2001**, *30*, 1305–1314. [[CrossRef](#)]

33. Bakhsh, A.; Kanwar, R.S.; Bailey, T.B.; Cambardella, C.A.; Karlen, D.L.; Colvin, T.S. Cropping system effects on NO<sub>3</sub>-N loss with subsurface drainage water. *Trans. ASAE* **2002**, *45*, 1789. [[CrossRef](#)]
34. Acharya, U.; Chatterjee, A.; Daigh, A.L.M. Effect of subsurface drainage spacing and depth on crop yield. *Agron. J.* **2019**, *111*, 1675–1681. [[CrossRef](#)]

**Disclaimer/Publisher’s Note:** The statements, opinions and data contained in all publications are solely those of the individual author(s) and contributor(s) and not of MDPI and/or the editor(s). MDPI and/or the editor(s) disclaim responsibility for any injury to people or property resulting from any ideas, methods, instructions or products referred to in the content.